Available online at www.sciencedirect.com
ScienceDirect
Phytochemistry 68 (2007) 2375–2392
PHYTOCHEMISTRY
www.elsevier.com/locate/phytochem

Kinetic model of sucrose accumulation in maturing sugarcane culm tissue

Lafras Uys [a], Frederik C. Botha [b,c], Jan-Hendrik S. Hofmeyr [a], Johann M. Rohwer [a,*]

[a] *Triple-J Group for Molecular Cell Physiology, Department of Biochemistry, Stellenbosch University, Private Bag X1, 7602 Matieland, South Africa*
[b] *South African Sugarcane Research Institute, Private Bag X02, 4300 Mount Edgecombe, South Africa*
[c] *Institute for Plant Biotechnology, Stellenbosch University, Private Bag X1, 7602 Matieland, South Africa*

Received 5 February 2007; received in revised form 11 April 2007
Available online 6 June 2007

Abstract

Biochemically, it is not completely understood why or how commercial varieties of sugarcane (*Saccharum officinarum*) are able to accumulate sucrose in high concentrations. Such concentrations are obtained despite the presence of sucrose synthesis/breakdown cycles (futile cycling) in the culm of the storage parenchyma. Given the complexity of the process, kinetic modelling may help to elucidate the factors governing sucrose accumulation or direct the design of experimental optimisation strategies.

This paper describes the extension of an existing model of sucrose accumulation (Rohwer, J.M., Botha, F.C., 2001. Analysis of sucrose accumulation in the sugar cane culm on the basis of *in vitro* kinetic data. Biochem. J. 358, 437–445) to account for isoforms of sucrose synthase and fructokinase, carbon partitioning towards fibre formation, and the glycolytic enzymes phosphofructokinase (PFK), pyrophosphate-dependent PFK and aldolase. Moreover, by including data on the maximal activity of the enzymes as measured in different internodes, a growth model was constructed that describes the metabolic behaviour as sugarcane parenchymal tissue matures from internodes 3–10.

While there was some discrepancy between modelled and experimentally determined steady-state sucrose concentrations in the cytoplasm, steady-state fluxes showed a better fit. The model supports a hypothesis of vacuolar sucrose accumulation against a concentration gradient. A detailed metabolic control analysis of sucrose synthase showed that each isoform has a unique control profile. Fructose uptake by the cell and sucrose uptake by the vacuole had a negative control on the futile cycling of sucrose and a positive control on sucrose accumulation, while the control profile for neutral invertase was reversed. When the activities of these three enzymes were changed from their reference values, the effects on futile cycling and sucrose accumulation were amplified.

The model can be run online at the JWS Online database (http://jjj.biochem.sun.ac.za/database/uys).

Keywords: Sugarcane; Kinetic modelling; Metabolic control analysis; Plant metabolism; Sucrose accumulation

1. Introduction

Commercial varieties of sugarcane (*Saccharum officinarum*) preferentially store sucrose in high concentrations, as opposed to starch. Dry matter accumulation and sucrose content increase sharply within the top internodes (Moore, 1995; Moore and Maretzki, 1996; Whittaker and Botha, 1997). The increase in sucrose content during internode maturation coincides with a repartitioning of carbon towards sucrose storage rather than insoluble matter and respiration (Whittaker and Botha, 1997). Moreover, in some varieties sucrose does not accumulate linearly with time, since the rate of accumulation increases significantly with internode maturity (Whittaker and Botha, 1997; Botha and Black, 2000). Although it is well known that significant differences in sucrose content are evident between, for example, ancestral and commercial sugarcane varieties, the biochemical basis for this is still poorly understood. If

* Corresponding author. Tel.: +27 21 808 5843; fax: +27 21 808 5863.
E-mail address: jr@sun.ac.za (J.M. Rohwer).

0031-9422/$ - see front matter © 2007 Elsevier Ltd. All rights reserved.
doi:10.1016/j.phytochem.2007.04.023

control points for this process could be identified, this would suggest rational experimental intervention strategies for maximising sucrose yield.

An important feature of the sucrose accumulation pathway in sugarcane culm is the pronounced futile cycling of sucrose. This is in part due to three known invertase isoforms that are present in storage parenchyma (Bosch et al., 2004; Hatch and Glasziou, 1963; Ma et al., 2000; Prado et al., 1980; Rose and Botha, 2000; Vattuone et al., 1981; Venkataramana et al., 1991; Vorster and Botha, 1998, 1999; Zhu et al., 1997), as well as the presence of enzymes such as sucrose synthase, which are readily reversible (Schäfer et al., 2004b). In an initial attempt to quantify the regulatory characteristics of this process and to identify control points, our group created a kinetic model of sucrose accumulation in the sugarcane culm (Rohwer and Botha, 2001). In line with experimental data, this model succinctly captured the futile cycling property and predicted approximately 22% of synthesised sucrose to be broken down again via this cycle. The model assumed that increased flux of sucrose into the vacuole should be followed by increased sucrose accumulation—to achieve this, a decrease in futile cycling was needed. The study concluded that increased specific activities of cytoplasmic glucose and fructose uptake, as well as of vacuolar sucrose uptake, should increase sucrose accumulation. Conversely, a decrease in neutral invertase activity should have the same effect.

Although our initial model (Rohwer and Botha, 2001) provided useful results, its construction was based on a number of simplifying—and potentially limiting—assumptions, including the following:

- the vacuole was not modelled as an explicit storage compartment,
- the levels of metabolic cofactors were clamped at experimentally determined concentrations,
- the model was restricted to internode 5 (numbered from the top of the plant) as representative of medium-mature (and thus developing) tissue,
- carbon partitioning towards fibre formation was not included,
- different enzyme isoforms were not considered explicitly, and catalysis was modelled as the implicit average of such isoforms when present and
- maximal activities of some enzymes were estimated due to lack of experimental data.

It is clear from the above that considerable scope exists for refinement and expansion of the model, and in this paper we present a more detailed and extended analysis. Based on our original model (Rohwer and Botha, 2001), maximal activities for the enzymes experimentally measured in tissues of varying stages of maturity (internodes 3–10) allowed us to build internode specific models and thus create a growth profile of metabolism around sucrose accumulation. A carbon utilisation branch towards fibre formation was also added. We subsequently used kinetic modelling to identify those reactions in the cytoplasm of the storage parenchyma that have the largest influence on sugarcane sucrose yield.

2. Building the kinetic model

This section describes in detail how the sucrose accumulation model was extended. For a general introduction to the methods used (steady-state kinetic modelling and control analysis), the reader is referred to Appendix A.

2.1. Stoichiometry

The model is described in terms of the mass transfer between metabolite pools (the stoichiometry), the rates of conversion from one metabolite to another (the rate equations and ODEs) and the "fixed" terms in the rate equations (the input parameters). The reaction scheme summarising the stoichiometry is shown in Fig. 1. The following are the most important extensions of the original model Rohwer and Botha, 2001:

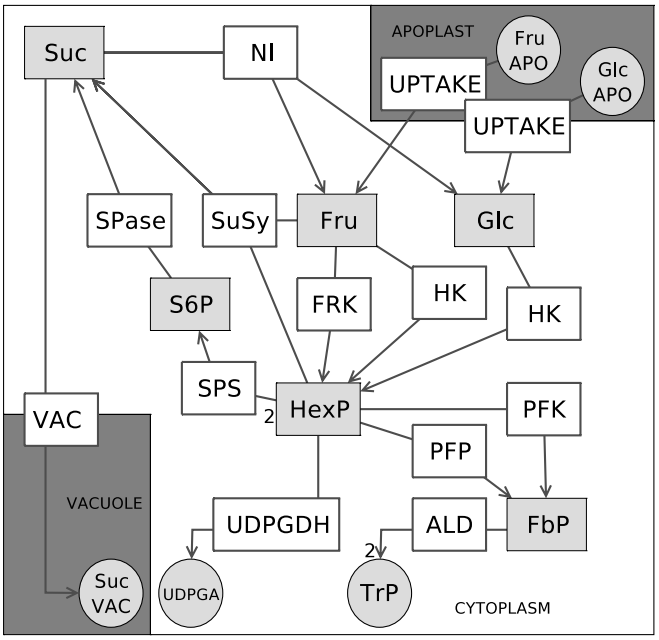

Fig. 1. Reaction scheme of the extended sucrose accumulation model. Metabolites are shaded in light grey and enclosed in rectangular boxes (variables) or circles (external fixed metabolites). Enzymes are enclosed in rectangular boxes without shading. A number 2 next to a line indicates a stoichiometric coefficient. *Abbreviations for enzymes and transport steps:* HK, Hexokinase; FRK, Fructokinase; UDPGDH, UDP-Glucose dehydrogenase; PFK, Phosphofructokinase; PFP, Pyrophosphate-dependent PFK; NI, Neutral invertase; SuSy, Sucrose synthase; ALD, Aldolase; SPS, Sucrose phosphate synthetase; SPase, Sucrose phosphatase; VAC, vacuolar sucrose import. *Metabolites:* Glc, Glucose; Fru, Fructose; Suc, Sucrose; S6P, Sucrose-6-phosphate; HexP, Hexose phosphate; FbP, Fructose-1,6-bisphosphate; UDPGA, UDP-Glucuronic acid; TrP, triose phosphate.

- Sucrose synthase (SuSy) and fructokinase (FRK) are modelled in terms of their respective isozymes as opposed to single reactions with averaged kinetic parameters.
- Rather than modelling a single glycolytic reaction from fructose-6-phosphate (F6P), partitioning to glycolysis now includes the phosphofructokinase (PFK)-pyrophosphate-dependent PFK (PFP) split and the aldolase (ALD)-catalysed draining reaction.
- UDP-glucose dehydrogenase (UDPGDH) drains hexose phosphates into UDP-glucuronic acid (UDPGA), the precursor for cell wall biosynthesis.

Neither the apoplast nor the vacuole is explicitly included in the model. This means that transport steps across these boundaries act as source and sink reactions for the system, and the corresponding source and sink metabolite concentrations are clamped in the model.

In keeping with the approach followed by Rohwer and Botha (2001), the interconversion of UDP-glucose (UDPGlc), F6P, glucose-6-phosphate (G6P) and glucose-1-phosphate (G1P) are modelled as a single equilibrium block, and values for these metabolite concentrations are calculated as fractions of the total hexose phosphate pool by using the equilibrium constants for the reactions.

2.2. Parameters

Model parameters can be divided into kinetic constants for the enzymes (e.g. Michaelis, inhibition or equilibrium constants), maximal activities of the various steps and the concentrations of external species. The latter, sometimes also referred to as "clamped" species, are typically the source and sink metabolites, which are assumed to be buffered by the system and are therefore fixed in the model to allow a steady-state to be calculated. Mathematically, they are boundary conditions for the system of ODEs.

Reported enzyme maximal activities show large variations. Ideally, all activities should be measured under identical circumstances and preferably in the same source tissue. Therefore, we aimed for as consistent a data set as possible by restricting ourselves to values reported from one laboratory. The enzyme maximal activities for the different internodes are listed in Table 3 and the conversion to a common unit is described in Appendix B.1. Consistency of the data is also further discussed in Section 3.5.

Kinetic constants were collected from a number of different literature sources and are listed in Table 4 and described in Appendix B.2. The clamped concentrations of all cofactors and external source metabolites are given in Table 5. Cofactors in the model (e.g. ATP and PP_i) are clamped and their regeneration is not modelled explicitly because of insufficient kinetic data for all the steps contributing to their regeneration. This is consistent with the approach followed in the original model and further detail is available in Rohwer and Botha (2001).

2.3. Availability

The model can be interrogated live on the JWS Online website (http://jjj.biochem.sun.ac.za/database/uys), requiring only a web browser. In addition, model definition files in PySCeS and SBML formats are available for download from the same URL.

3. Model analysis and discussion

This section deals first with a comparison of the state variables as predicted by the model to independent experimental literature data. Next, the metabolic changes associated with internode maturation are explored, and we investigate in detail the control exercised by the SuSy isozymes over the reactions and metabolite concentrations. Finally, parameter scans are performed for maximal activities of enzymes that have the greatest effect on futile cycling of sucrose to establish the effect on sucrose accumulation rate. A general discussion places our results in the context of existing knowledge.

3.1. Comparison to experimental data

Comparisons of the model-predicted steady-state flux and concentration values to experimental data are given in Figs. 2 and 3. Measurements of carbon partitioning in sugarcane storage tissue (Bindon and Botha, 2002) were used for the comparison with simulated flux values. These experiments analysed steady-state labelling in tissue discs, where steady-state conditions may thus be assumed to hold. Furthermore maximal activity data was obtained from *in vitro* assays of sugarcane tissue of a particular internode (i.e. maturity). Since the time-scale of growth is much slower than that covered by the metabolic model, the steady-state comparison is again valid (see also Appendix A.2). Experimental flux values were only reported for internodes 3, 5 and 9; values for internodes 4, 6, 7 and 8 were obtained from a spline interpolation, which was used as a first approximation for the missing data. An artificial data point (0.1× the predictor for internode 9) was introduced for a fictitious internode 20 to anchor the spline. All predictor data were present in the spline values correct to an accuracy of approximately 1% or better.

Data are presented as a ratio between glycolytic, storage or fibre fluxes and flux of glucose uptake. The version of the model used to validate the fluxes had the maximal activity of fructose uptake set to 10^{-6} mM min^{-1} (effectively zero) to mimic the experimental protocol, in which only radiolabelled glucose was fed to tissue disks. A value of 10^{-6} mM min^{-1} was used, rather than absolute zero, to ensure the numerical stability of the solver algorithms. The good correlation between experimental and modelled flux values for UDPGDH is due to the fact that the experimental data were used to estimate a V_{max} value for UDPGDH (see also Appendix B.1). Flux ratios for $\frac{J_{VAC}}{J_{up}^{Glc}}$ did not

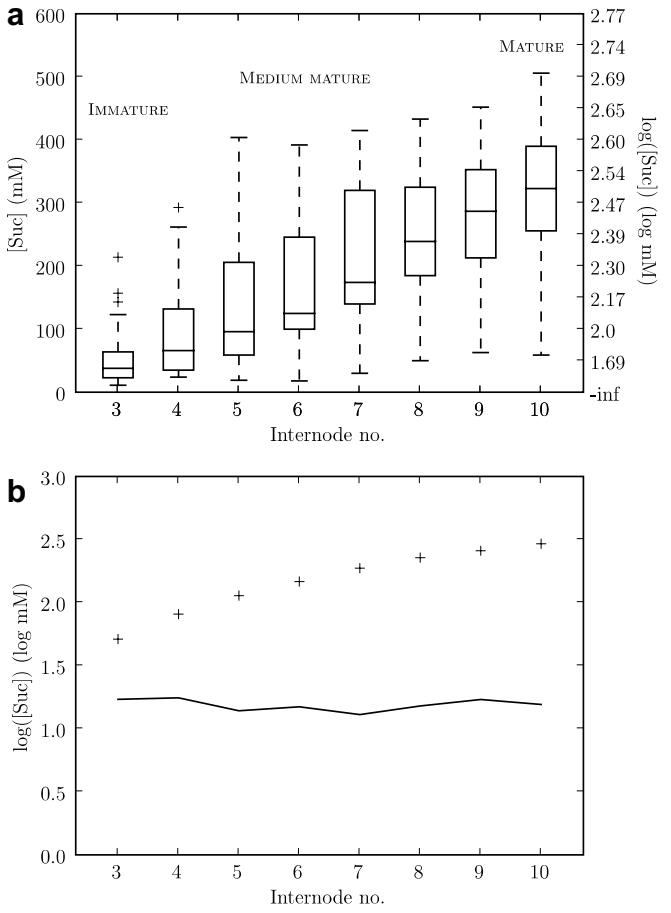

Fig. 2. Test set of experimentally determined sucrose concentrations and comparison of model-predicted sucrose concentrations with experimental data. (a) Boxplot of sucrose levels in the culm tissue of various internodes. Data were collected from Bindon and Botha (2002), Bosch (2005), Bosch et al. (2004), Botha and Black (2000), Botha et al. (1996), Glasziou (1960), Komor (1994), Rae et al. (2005), Rose and Botha (2000), Walsh et al. (2005), Whittaker and Botha (1997) and Zhu et al. (1997), representing different varieties, seasonal and environmental conditions. The data were converted to a common unit and pooled (Uys, 2006). The centre line indicates the median value, the box the first and third quartile, and the whiskers extend to the most extreme values in the range 1.5× the range of the box. Outliers are indicated by +. (b) Comparison of model outputs (solid line) with experimental data (+).

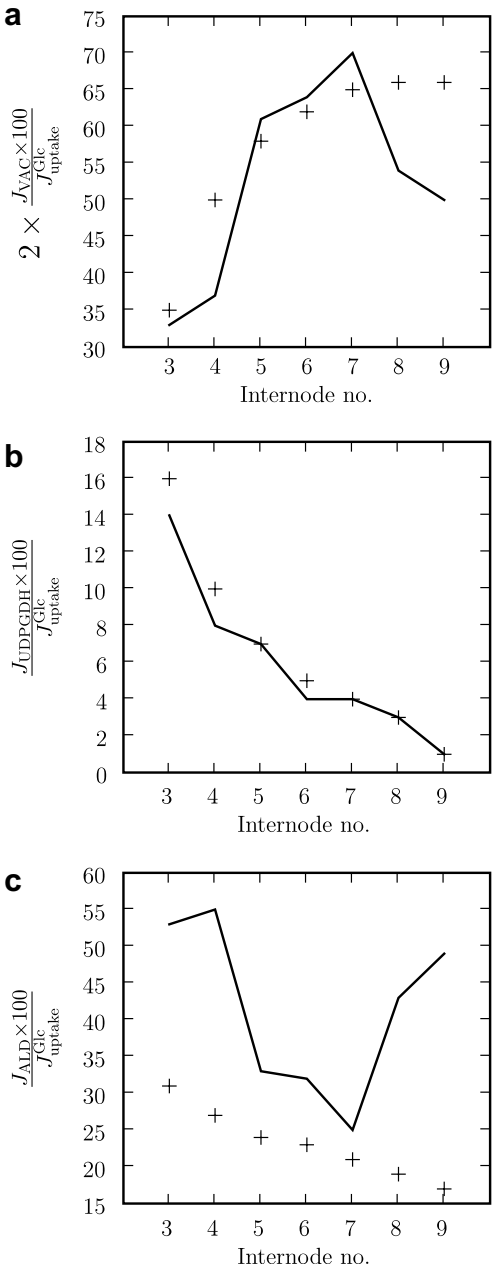

Fig. 3. Comparison of model-predicted flux ratios (solid line) with experimental data (+). (a)–(c) Various flux ratios, experimental data from Bindon and Botha (2002).

correlate well with experimental data. The reason for this is not immediately clear; however, it is possible that the model underestimates sucrose flux into the vacuole and overestimates flux into glycolysis. The model-predicted flux values always add up to 100%, because these three reactions are the only sink reactions present in the model and therefore represent the total flux out of the system. An unaccounted for sink reaction or non-steady-state conditions in the experimental set-up could also contribute to the disparity. Importantly, models that do not exactly predict experimental fluxes and concentrations may still be useful. For example, the overall dynamic behaviour of a model can still be captured and its control properties can be calculated.

The comparison of experimental and simulated sucrose concentrations is shown in Fig. 2. If one assumes that the measurement of sucrose concentrations in each sugarcane internode is a snapshot of a prevailing quasi-steady-state, then a comparison of model-predicted steady-state values using maximal activities measured in that internode should be justified. Nevertheless, the comparison is slightly misleading, because

- the model only predicts sucrose concentrations *in the cytoplasm*, whereas
- the experimentally determined sucrose concentrations account for sucrose in the entire *internodal volume*, i.e. sucrose in the cytoplasm, apoplast, vacuole, phloem and other compartments.

We make the comparison to point out that if the model is correct then sucrose should not accumulate in the cytoplasm because the expected sucrose concentrations are much higher than those predicted by the model. This point is discussed extensively in Section 3.6.

3.2. Modelling sugarcane growth

In order to investigate metabolic changes that occur during the maturation process of sugarcane culm tissue, we prepared a set of eight models, representative of internodes

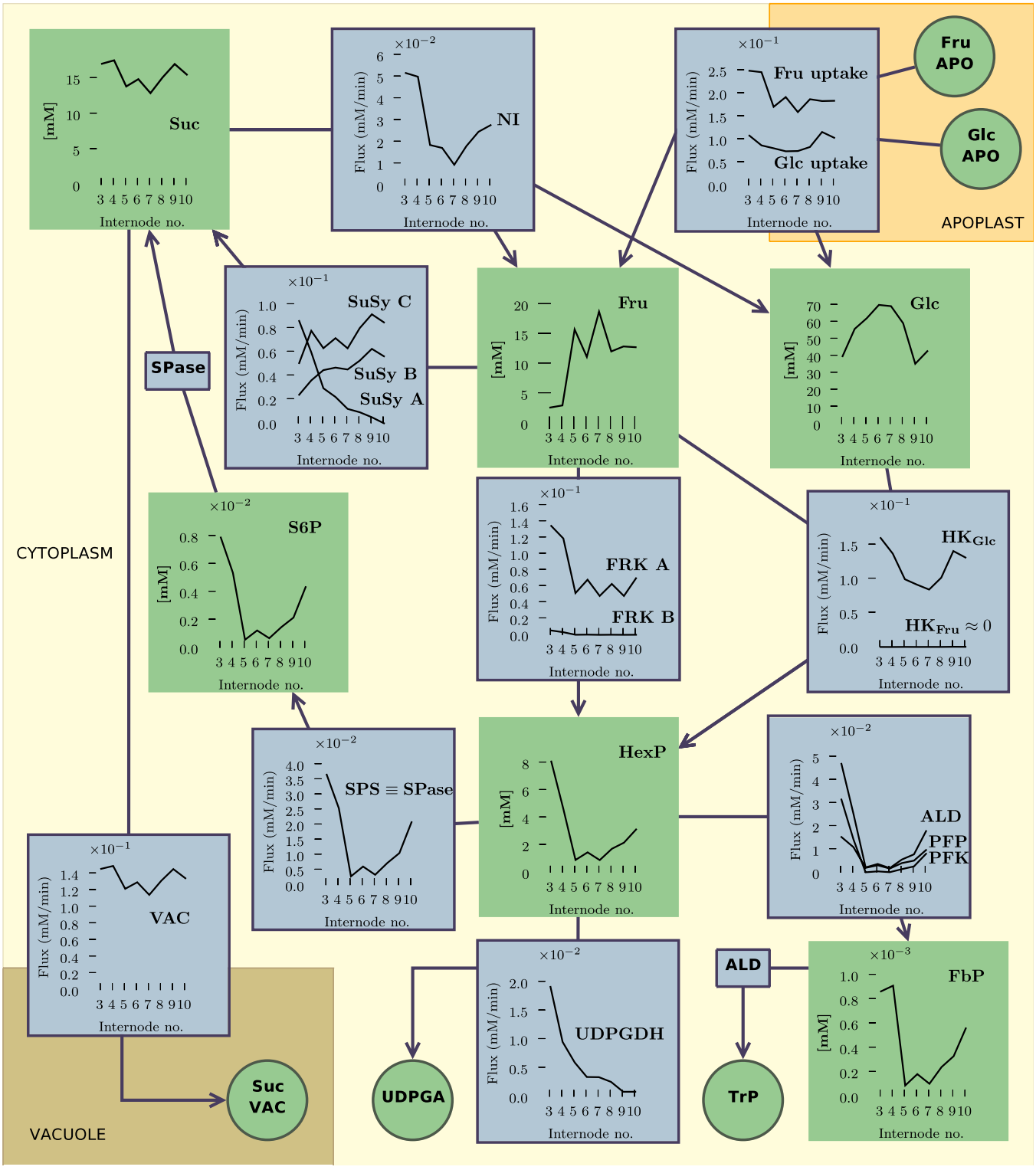

Fig. 4. Steady-state properties of the model for internodes 3–10. Fluxes are shown with a blue background, steady-state concentrations with a green background. The figure follows the same layout as the reaction scheme in Fig. 1.

3–10, by substituting the internode-specific maximal enzyme activities and isozyme-specific expression profiles (where available) into the model parameter set. The resulting steady-state properties are summarised in Fig. 4. In addition, we calculated the pairwise Pearson linear correlation coefficients for the steady-state variables over the eight different internodes (Table 1). Correlation between data sets does not imply causation; however, correlation coefficients are valuable as a means of exploring large data sets to detect trends. In this particular case correlation coefficients were calculated to see how steady-state variables changed in relation to other variables with increasing internode maturity. Due to the highly non-linear nature of metabolic pathways, linear correlations are not necessarily expected and strong linear correlations, where seen, may warrant further investigation. The following list discusses some of the features of the correlation coefficients in Table 1.

(1) Fructose (Fru) and glucose (Glc) concentrations correlate negatively with every other metabolite except with each other. This comes as no surprise, as the model only has Fru and Glc to act as carbon source. Care should be taken when interpreting concentration–concentration correlation coefficients. A negative correlation coefficient means that if one quantity decreases the other increases. This can only be true for Fru and Glc if they are actually converted to some other molecule. Considering fluxes, if the flow of carbon into the cell decreases one expects the other metabolites in the cell to decrease to some

Table 1
Pairwise Pearson correlation coefficients for steady-state fluxes and concentrations of all eight internodes

	Fru	Glc	S6P	Suc	FbP	UDPGlc	G1P	G6P	F6P
Fru	1.00								
Glc	0.38	1.00							
S6P	−0.85	−0.64	1.00						
Suc	−0.85	−0.71	0.76	1.00					
FbP	−0.88	−0.58	0.95	0.83	1.00				
UDPGlc	−0.87	−0.6	0.98	0.74	0.89	1.00			
G1P	−0.87	−0.6	0.98	0.74	0.89	1.00	1.00		
G6P	−0.87	−0.6	0.98	0.74	0.89	1.00	1.00	1.00	
F6P	−0.87	−0.6	0.98	0.74	0.89	1.00	1.00	1.00	1.00
J^{Fru}_{uptake}	−0.99	−0.36	0.86	0.82	0.89	0.89	0.89	0.89	0.89
J^{Glc}_{uptake}	−0.33	−0.99	0.6	0.68	0.53	0.56	0.56	0.56	0.56
J^{Glc}_{HK}	−0.73	−0.9	0.88	0.88	0.85	0.86	0.86	0.86	0.86
J^{Fru}_{HK}	0.54	−0.51	−0.27	−0.05	−0.29	−0.36	−0.36	−0.36	−0.36
$J_{FRK\,A}$	−0.95	−0.31	0.91	0.7	0.9	0.93	0.93	0.93	0.93
$J_{FRK\,B}$	−0.89	−0.36	0.88	0.65	0.82	0.94	0.94	0.94	0.94
J_{SPS}	−0.85	−0.65	1.00	0.77	0.96	0.97	0.97	0.97	0.97
J_{SPase}	−0.85	−0.65	1.00	0.77	0.96	0.97	0.97	0.97	0.97
$J_{SuSy\,A}$	−0.83	−0.14	0.72	0.52	0.68	0.81	0.81	0.81	0.81
$J_{SuSy\,B}$	0.66	−0.01	−0.59	−0.23	−0.51	−0.69	− 0.69	−0.69	−0.69
$J_{SuSy\,C}$	0.2	−0.29	−0.24	0.24	−0.06	−0.37	−0.37	−0.37	−0.37
J_{NI}	−0.94	−0.55	0.93	0.85	0.96	0.92	0.92	0.92	0.92
J_{PFP}	−0.84	−0.55	1.00	0.77	0.96	0.96	0.96	0.96	0.96
J_{PFK}	−0.83	−0.56	0.96	0.67	0.87	0.99	0.99	0.99	0.99
J_{ALD}	−0.85	−0.6	0.98	0.71	0.9	1.00	1.00	1.00	1.00
J_{UDPGDH}	−0.76	−0.21	0.74	0.45	0.63	0.85	0.85	0.85	0.85
J_{VAC}	−0.85	−0.71	0.76	1.00	0.83	0.74	0.74	0.74	0.74

	J^{Fru}_{uptake}	J^{Glc}_{uptake}	J^{Glc}_{HK}	J^{Fru}_{HK}	$J_{FRK\,A}$	$J_{FRK\,B}$	J_{SPS}	J_{SPase}	$J_{SuSy\,A}$	$J_{SuSy\,B}$	$J_{SuSy\,C}$	J_{NI}	J_{PFP}	J_{PFK}	J_{ALD}	J_{UDPGDH}	J_{VAC}
J^{Fru}_{uptake}	1.00																
J^{Glc}_{uptake}	0.31	1.00															
J^{Glc}_{HK}	0.72	0.87	1.00														
J^{Fru}_{HK}	−0.58	0.55	0.11	1.00													
$J_{FRK\,A}$	0.97	0.26	0.69	−0.64	1.00												
$J_{FRK\,B}$	0.93	0.33	0.71	−0.59	0.96	1.00											
J_{SPS}	0.86	0.6	0.88	−0.27	0.9	0.87	1.00										
J_{SPase}	0.86	0.6	0.88	−0.27	0.9	0.87	1.00	1.00									
$J_{SuSy\,A}$	0.88	0.11	0.53	−0.72	0.9	0.95	0.71	0.71	1.00								
$J_{SuSy\,B}$	−0.72	0.13	−0.28	0.83	−0.81	−0.86	−0.58	−0.58	−0.94	1.00							
$J_{SuSy\,C}$	−0.28	0.3	0.06	0.67	−0.42	−0.55	−0.22	−0.22	−0.67	0.85	1.00						
J_{NI}	0.95	0.5	0.86	−0.38	0.94	0.91	0.93	0.93	0.83	−0.64	−0.21	1.00					
J_{PFP}	0.85	0.62	0.89	−0.24	0.89	0.85	1.00	1.00	0.68	−0.54	−0.19	0.93	1.00				
J_{PFK}	0.86	0.52	0.82	−0.39	0.92	0.95	0.96	0.96	0.83	−0.74	−0.46	0.9	0.95	1.00			
J_{ALD}	0.87	0.56	0.85	−0.35	0.92	0.93	0.98	0.98	0.8	−0.69	−0.38	0.92	0.97	0.99	1.00		
J_{UDPGDH}	0.81	0.18	0.55	−0.65	0.87	0.96	0.73	0.73	0.97	−0.94	−0.75	0.78	0.7	0.88	0.84	1.00	
J_{VAC}	0.81	0.68	0.88	−0.04	0.7	0.65	0.77	0.77	0.52	−0.22	0.25	0.85	0.77	0.67	0.71	0.45	1.00

extent, which would require the coefficient to be positive. This is supported by the positive correlation coefficients between $J^{\mathrm{Fru}}_{\mathrm{uptake}}$ and $J^{\mathrm{Glc}}_{\mathrm{uptake}}$ and all the metabolites except Fru and Glc. The negative correlations between $J^{\mathrm{Fru}}_{\mathrm{uptake}}$ and $J^{\mathrm{Glc}}_{\mathrm{uptake}}$ on the one hand and Fru and Glc on the other can be explained by the feedback inhibition of the intracellular sugars on their respective uptake steps.

(2) Metabolites of the hexose phosphate pool, excluding fructose-1,6-bisphosphate (FbP), all have identical correlation profiles since the model assumes that these species are in equilibrium. Sucrose-6-phosphate (S6P) is almost completely linearly correlated to the hexose phosphate pool for two reasons: first, S6P is only synthesised from hexose phosphates, and second, the sucrose phosphate synthase (SPS) reaction makes only the one product (S6P), which in turn is the sole substrate for sucrose phosphatase (SPase) and no other reactions (Fig. 4). Thus, if the hexose phosphate concentration increases then the SPS flux will increase and more S6P will be formed. S6P is negatively correlated to sucrose (Suc), since dephosphorylation of S6P yields Suc.

(3) J_{VAC} is completely positively correlated to Suc. This is expected, since the vacuolar sucrose uptake rate equation is a function of Suc only. The strongest correlation of Suc, after J_{VAC}, is to $J_{\mathrm{SuSy\,A}}$ and $J_{\mathrm{SuSy\,C}}$. The correlation with $J_{\mathrm{SuSy\,C}}$ is as expected, since of the sucrose synthesising enzymes, $J_{\mathrm{SuSy\,C}}$ carries by far the largest steady-state flux. From this it can be inferred that the synthesis and storage of sucrose is mostly dependent on SuSy C.

3.3. Control by SuSy isozymes

One of the main extensions of the current model compared to the original version in Rohwer and Botha (2001) is the explicit modelling of the isozymes of SuSy and FRK (see Section 2.1). Hence, we calculated the control coefficient of each of the three SuSy isozymes on all the

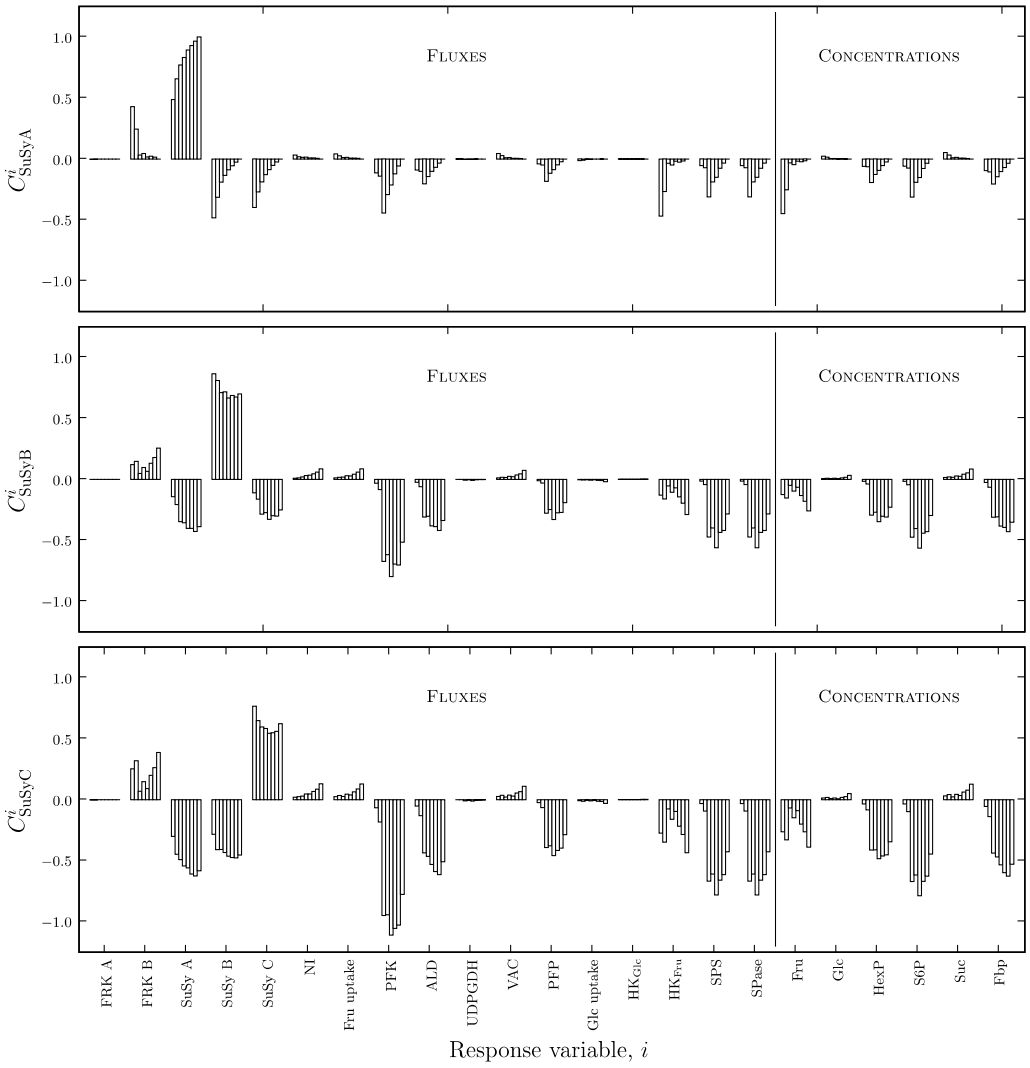

Fig. 5. Flux- and concentration-control coefficients of SuSy A, B & C as calculated by the model. For each model variable on the *X*-axis, the control coefficients are shown by a series of eight bar graphs representing internodes 3–10.

model variables (Fig. 5). The three isozymes had the most control over themselves and negative control over each other. This is not really surprising since they all compete for the same substrate. It would also explain why all three enzymes had negative control over flux through fructose-phosphorylating hexokinase. In all cases the relationship

$$C^{J_x}_{\text{SuSy A}} : C^{J_x}_{\text{SuSy B}} : C^{J_x}_{\text{SuSy C}} = J_{\text{SuSy A}} : J_{\text{SuSy B}} : J_{\text{SuSy C}} \quad (1)$$

held true, where J_x is any steady-state flux other than through the SuSy isozymes. Thus, the amount of control by an enzyme over the fluxes and concentrations in a system is shared by the isoforms of that enzyme, and moreover, the size of the fraction of that control residing in an isoform is proportional to the flux carried by that isoform.

3.4. Control analysis of sucrose accumulation

Metabolic control analysis (MCA) allows us to identify those reactions with the greatest control on the flux of sucrose accumulation into the vacuole. With a kinetic model, the effect of changing the levels of these enzymes can be investigated. In Rohwer and Botha (2001) we argued that futile cycling of sucrose is an energetically expensive process that decreases the amount of sucrose available for partitioning into storage. The control of this process was investigated by defining a futile cycling control coefficient (FCCC) as $C_i^{J_{\text{NI}}/J_{\text{VAC}}}$ (Rohwer and Botha, 2001), which quantifies the extent to which a reaction can increase or decrease the flux ratio of vacuolar sucrose accumulation to breakdown by neutral invertase. The smaller $J_{\text{NI}}/J_{\text{VAC}}$ is, the more sucrose is being stored as opposed to being broken down. It would therefore be valuable to know which enzymes have the largest effect on this value, as they would constitute good candidates for biotechnological manipulation to increase sucrose yield. FCCCs of all the enzymes were calculated for all eight internodes (Table 2). The results obtained for each internode do not differ significantly from the original model of Rohwer and Botha (2001). Glc_{up}, Fru_{up} and VAC retained the largest negative impact on futile cycling, while HK_{Glc} and NI were still the main contributors to futile cycling. The analysis of FCCCs also shows that the control over futile cycling does not shift drastically with internode maturity, and we conclude that the same enzymes are responsible for futile cycling regardless of physiological changes due to internodal tissue maturation.

$v^{\text{Glc}}_{\text{HK}}$ and v_{NI} had the largest positive control over $J_{\text{NI}}/J_{\text{VAC}}$, whereas $v^{\text{Glc}}_{\text{uptake}}$, $v^{\text{Fru}}_{\text{uptake}}$ and v_{VAC} had the largest negative control (Table 2). These two groups of antagonistic enzymes were chosen for *in silico* manipulation of their levels. Increasing concentrations of enzymes with large negative control over futile cycling should lead to a decrease in futile cycling, while the converse is true for enzymes with large positive control. Hence, the given maximal activity of NI was decreased and those of Fru_{up} and VAC were increased in the model. Steady-state solutions were calculated as these enzymes were incremented five-fold from their initial reference values (Fig. 6). Similar to Rohwer and Botha (2001), futile cycling was found to decrease and the conversion ratio of hexoses to sucrose remained virtually constant over all the manipulations. The flux of sucrose into the vacuole increased with all the changes made. It is expected that all species concentrations should respond to such an alteration in the maximal activity of an enzyme, including, for example, cofactor concentrations. The fact that cofactors are clamped at constant concentrations in our model is thus a simplifying, albeit necessary, assumption, since to our knowledge these analyses have not yet been performed *in vivo*. The fact that none of the manipulated enzymes has any direct cofactor dependence may mitigate this simplification.

Table 2
Futile cycling control coefficients, defined as $C_i^{J_{\text{NI}}/J_{\text{VAC}}}$ (see text), for all eight internodes in order of increasing magnitude of the mean

Perturbation	Internode (*i*)								Mean	s.d.	Slope
	3	4	5	6	7	8	9	10			
V^{Glc}_{up}	−0.802	−0.748	−0.904	−0.905	−0.976	−0.927	−0.971	−0.917	−0.894	0.079	−0.024
V^{Fru}_{up}	−0.768	−0.69	−0.622	−0.582	−0.692	−0.58	−0.537	−0.548	−0.627	0.081	0.028
V_{VAC}	−0.341	−0.328	−0.535	−0.494	−0.611	−0.504	−0.487	−0.489	−0.474	0.095	−0.022
V_{SPS}	−0.069	−0.036	−0.01	−0.012	−0.017	−0.016	−0.021	−0.036	−0.027	0.02	0.003
$V_{\text{SuSy A}}$	−0.013	−0.009	0.004	0.003	0.004	0.002	0.001	0	−0.001	0.006	0.002
V_{SPase}	−0.002	0	0	0	0	0	0	0	0	0.001	0
V_{ALD}	0	0.001	0	0	0	0	0	0	0	0	0
$V^{\text{Fru}}_{\text{HK}}$	0	0	0.001	0	0.001	0	0.001	0.001	0	0	0
$V_{\text{FRK B}}$	0.01	0.004	0.001	0.001	0.001	0.001	0	0	0.002	0.003	−0.001
V_{UDPGDH}	0.025	0.015	0.002	0.004	−0.002	0.002	0.001	0.001	0.006	0.009	−0.003
V_{PFP}	0.02	0.017	0.001	0.003	−0.001	0.004	0.005	0.011	0.007	0.008	−0.001
$V_{\text{SuSy B}}$	−0.003	−0.006	0.006	0.007	0.015	0.011	0.017	0.017	0.008	0.009	0.003
$V_{\text{SuSy C}}$	−0.007	−0.011	0.008	0.01	0.019	0.015	0.022	0.022	0.01	0.013	0.005
V_{PFK}	0.041	0.023	0	0.001	0	0.001	0.003	0.01	0.01	0.015	−0.004
V_{FRKA}	0.24	0.149	0.172	0.138	0.24	0.141	0.101	0.134	0.164	0.051	−0.012
V_{NI}	0.692	0.658	0.796	0.806	0.868	0.814	0.811	0.782	0.778	0.069	0.018
$V^{\text{Glc}}_{\text{HK}}$	0.976	0.962	1.08	1.021	1.152	1.037	1.055	1.011	1.037	0.061	0.008

The slope is the first derivative of a linear regression line and gives an indication by how much a coefficient changes with internode maturity.

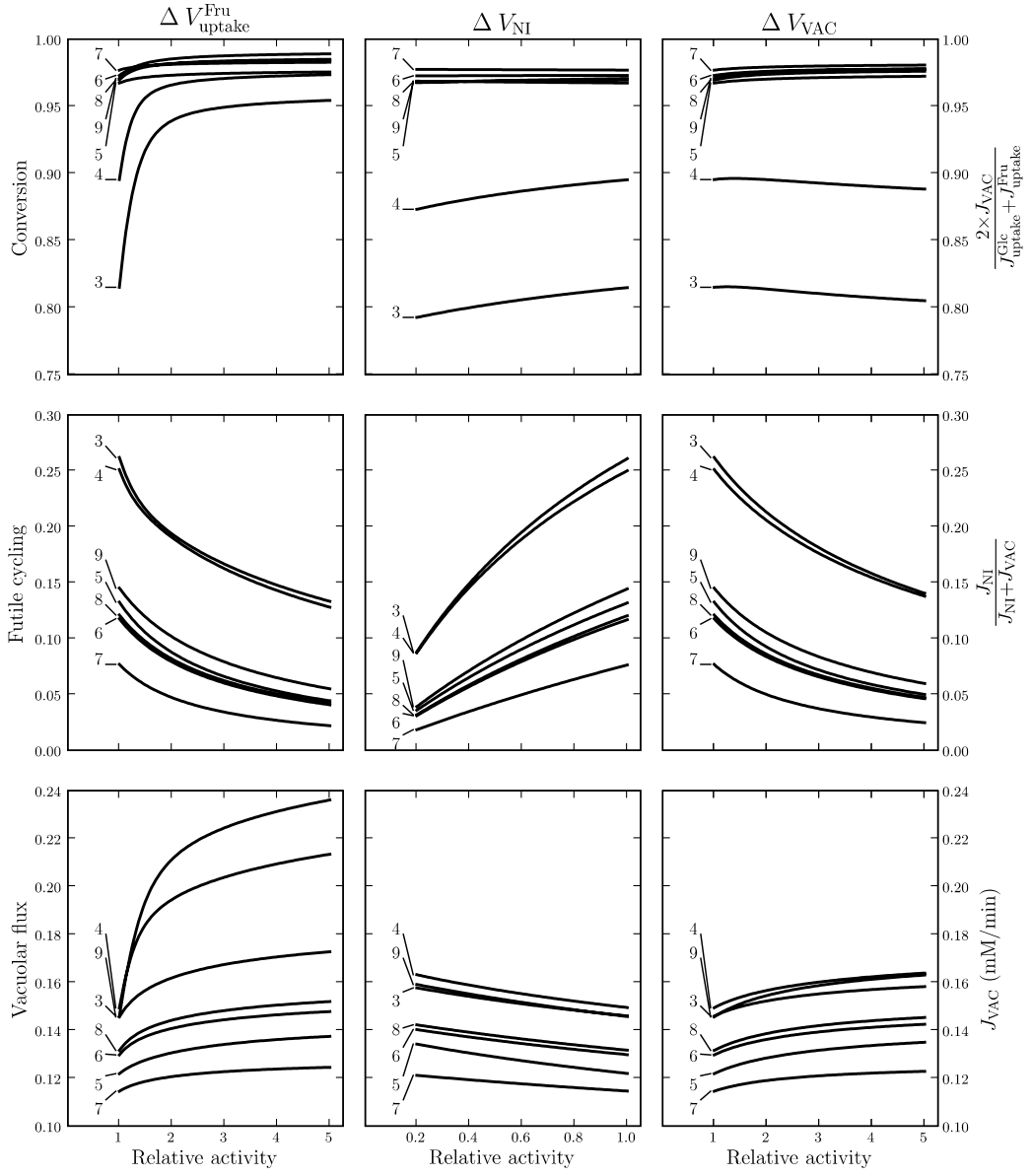

Fig. 6. Parameter scans depicting conversion efficiency, futile cycling and vacuolar uptake flux of sucrose (defined mathematically as on the right-hand *Y*-axis) in response to an increase in the maximal activities of Fru_{up} and VAC to five times their reference values, and attenuation of NI maximal activity to 20% of its reference value. Line labels refer to internode numbers.

3.5. Evaluation of the model

If we assume that the sucrose concentration should be equal between apoplast, symplast and vacuole, then approximately one to two-fold higher sucrose concentrations are expected in the more mature internodes (internodes 6 and up) than predicted by the model (Fig. 2, see also Welbaum and Meinzer, 1990). The following list discusses some problems that could have led to erroneous results.

(1) The maximal velocities entered into the model (Table 3) may not be an accurate reflection of reality. In kinetic studies that focused on only a few enzymes, notably larger specific maximal velocities were reported when compared to attempts to assay many enzymes simultaneously. We calculated a maximal activity of 0.925 mM min^{-1} for FRK A and 0.677 mM min^{-1} for FRK B for internode 5, based on a study that focused only on fructokinase (Hoepfner and Botha, 2003). In contrast, the dataset used in the model has values of 0.059 and 0.042 mM min^{-1} for FRK A and FRK B, respectively. These values are from a study that assayed 11 enzymes (Botha et al., 1996). Clearly there is a difference of more than one order of magnitude between the focused and broader investigations, and this is but one example of the disparity found between various reported enzyme maximal activities. In our model we used the maximal activity values from the broader study (Botha et al., 1996) in order to reduce or eliminate

Table 3
Maximal activities in mM min^{-1} for all enzymes and transport steps in the model for each internode

Enzyme	Internode (*i*)								References
	3	4	5	6	7	8	9	10	
V^{Fru}_{uptake}	0.286	0.286	0.286	0.286	0.286	0.286	0.286	0.286	Rohwer and Botha (2001)
V^{Glc}_{uptake}	0.286	0.286	0.286	0.286	0.286	0.286	0.286	0.286	
V_{VAC}	1.000	1.000	1.000	1.000	1.000	1.000	1.000	1.000	
V_{SPase}	0.500	0.500	0.500	0.500	0.500	0.500	0.500	0.500	
V_{fSPS}	0.205	0.252	0.263	0.269	0.317	0.253	0.266	0.325	Botha (p.c.)
V_{rSPS}	0.108	0.133	0.139	0.142	0.167	0.134	0.140	0.171	
V^{Glc}_{HK}	0.204	0.173	0.125	0.115	0.106	0.128	0.178	0.166	
V^{Fru}_{HK}	0.204	0.173	0.125	0.115	0.106	0.128	0.178	0.166	
V_{NI}	0.320	0.399	0.238	0.213	0.147	0.197	0.174	0.235	Botha et al. (1996)
V_{PFP}	0.375	0.410	0.322	0.316	0.277	0.355	0.363	0.499	
V_{PFK}	0.189	0.272	0.132	0.143	0.168	0.265	0.278	0.365	
V_{ALD}	0.862	0.442	0.379	0.310	0.288	0.357	0.366	0.498	
$V_{FRK\ A}$	0.155	0.137	0.059	0.078	0.055	0.072	0.055	0.080	Botha et al. (1996), allocation to isoforms discussed in text
$V_{FRK\ B}$	0.171	0.118	0.042	0.048	0.030	0.035	0.024	0.032	
$V_{SuSy\ A}$	0.163	0.156	0.077	0.047	0.028	0.016	0.007	0.000	
$V_{SuSy\ B}$	0.109	0.184	0.145	0.137	0.130	0.130	0.130	0.095	
$V_{fSuSy\ C}$	0.109	0.184	0.145	0.137	0.130	0.130	0.130	0.095	
$V_{rSuSy\ C}$	0.256	0.431	0.340	0.323	0.305	0.306	0.306	0.224	
V_{UDPGDH}	0.022	0.011	0.007	0.004	0.004	0.003	0.001	0.001	Estimate

The origin of this data is discussed in the text.
p.c. – private communication.

many of the possible causes that give rise to variations in enzyme assays. Specifically, this study used data

- for plant samples from the same sugarcane variety and possibly even from the same plant,
- where assay conditions were kept relatively similar for all the enzyme assays and,
- where assays were performed in the same laboratory by one group of investigators.

Furthermore, the values reported in Botha et al. (1996) included maximal activities for almost all immature to mature internodes. These considerations outweighed the choice to select values from more focused studies. While focused studies may individually perhaps be more accurate, their assay conditions are in most cases incompatible with assay conditions for other enzymes.

(2) Inhibition of PFK by ATP and PFP by inorganic phosphate may play a role in the degree to which carbon is partitioned to glycolysis. Both ATP and inorganic phosphate concentrations were clamped in the model resulting in static inhibitory effects on these enzymes, and control of fluxes and concentrations by these enzymes. These metabolites were kept constant because no acceptable kinetic data were found for the regeneration of ATP and inorganic phosphate. The reactions could therefore not be modelled, and it was assumed that the model was not limited by the regeneration of either of these species. If, for example, the inorganic phosphate concentration had been free to vary, then the flux to glycolysis would have run dry, because it would have been used up as a substrate if not replenished.

(3) Some kinetic parameters were estimated from measurements of related enzymes in other plant species. Steady-state solutions are sometimes sensitive to small changes in parameters. Future refinements of the model could be able to correct this by including parameter values measured in sugarcane. As an example, we calculated the response coefficient (see

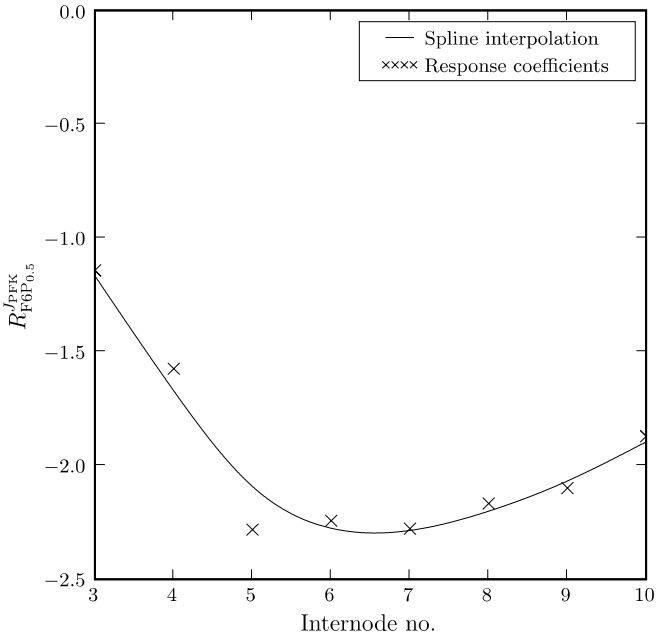

Fig. 7. Response coefficients ($R^{J_{PFK}}_{F6P_{0.5}}$) of the half saturation constant for PFK with respect to F6P ($F6P_{0.5}$) on the flux through PFK (J_{PFK}) plotted against internode number.

Appendix A.3) of the flux through PFK (J_{PFK}) with respect to a change in the half-saturation constant of PFK for F6P ($F6P_{0.5}$). Fig. 7 shows how $R^{J_{PFK}}_{F6P_{0.5}}$ changes with internode number. For example, in internode 5, $R^{J_{PFK}}_{F6P_{0.5}} = -2.24$. This means that a 10% change in the value of $F6P_{0.5}$ should lead to an almost 22% decrease in J_{PFK}. This sort of amplification of a small change in a parameter into a larger change in a steady-state variable means that care must be taken with the selection of parameter values.

(4) In our model, sugar uptake is restricted to fructose and glucose, though it has been shown that sugarcane tissue disks are able to take up sucrose (Komor, 2000a,b; Komor et al., 1981; Titus, 2005). The mechanism by which this occurs is not yet clear. We attempted to include this data into the sucrose accumulation model, but were unable to obtain biologically feasible steady-state solutions (data not shown). Introducing an extra source of sucrose in the model could possibly change the cytoplasmic sucrose profile of the maturing internodes.

(5) There are possibly three isoforms of hexokinase (Hoepfner and Botha, 2004). It is conceivable that kinetic parameters would differ depending on whether fructose or glucose is phosphorylated. Other enzymes may also well be present in different isoforms. Explicitly modelling SuSy and FRK isozymes has shown that this can affect steady-state model solutions—the control profile of the SuSy isozymes is given as an example (Fig. 5). Most importantly, the control of an enzyme is not equally distributed between isoforms, and the control distribution may shift with physiological conditions. It is expected that if hexokinase, or any other enzyme for that matter, is modelled in terms of its isoforms, a metabolic control analysis would pinpoint which isozymes have significant effects on sucrose accumulation.

3.6. The case for vacuolar sucrose uptake

The experimental sucrose concentrations in Fig. 2 show a linear increase of the mean sucrose concentration as internodes mature. From internodes 3–10, this gradient is about 39 mM internode^{-1}. In other words, the total sucrose concentration increases by about 34% per internode as culm tissue matures. In contrast, the model showed virtually constant sucrose concentrations across all the internodes. A comparable percentage increase in simulated sucrose concentrations was therefore not observed. So the question is, where is the sucrose? If the majority of the sucrose is not in the cytoplasm, it has to be either in the vacuole or the apoplast. The pairwise Pearson correlation coefficient of Suc with J_{VAC} is 1.0 (Table 1). From this it can be inferred that any increase in Suc will lead to an increase in the rate at which Suc is accumulating in the vacuole. An increase in J_{VAC} with Suc is not surprising, as vacuolar sucrose uptake is modelled with irreversible Michaelis–Menten kinetics (see Appendix C for discussion on this choice of rate equation), making the flux directly dependent on Suc. This may well be a simplification, and a clearer conception is needed of what exactly the mechanism is of sucrose uptake across the tonoplast.

The modelling results show that Glc and Fru concentrations remain higher than those of sucrose (Fig. 4). Since there is net synthesis of sucrose, removal from the cytoplasmic compartment has to exist, otherwise higher cytoplasmic Suc concentrations should be seen. High precursor and low product concentrations would favour sucrose synthesis, so higher Glc and Fru concentrations can be expected to support net sucrose synthesis. It has been shown that vacuoles can accumulate sugars other that sucrose (Preisser and Komor, 1991); however, our model does not specifically account for this. The only way that carbohydrates can be mobilised from the vacuole is by breakdown of vacuolar sucrose into glucose and fructose. It is unlikely that a large concentration gradient would exist between vacuolar and cytoplasmic glucose and fructose. It can be hypothesised that this state of affairs sustains the cytoplasmic synthesis of sucrose and immediate accumulation thereof in the vacuole.

Sucrose can enter an internode in one of three ways: from leaves attached to a node, or via vascular tissue from the less mature internodes above, or more mature internodes below. The sucrose from internodes below can be assumed to contribute to total internodal sucrose accumulation if sucrose unloading further down the plant is saturated. Incident radiation from sunlight decreases with canopy depth and increases with leaf size. The rate of sucrose unloading by the leaves per internode might thus be assumed to remain relatively constant. An internode does not retain all the sucrose that passes by in the phloem; it follows that the amount of sucrose available for uptake increases with internode maturity. This increased supply of sucrose is not reflected in our model, as it should lead to an increased supply of apoplastic glucose and fructose through the action of acid wall invertase for the more mature internodes; however, for lack of more specific data, apoplastic glucose and fructose are clamped at 5 mM for all internodes. The cytoplasmic sucrose concentration does not increase significantly, leaving only the vacuole and the apoplastic space to store sucrose (Welbaum and Meinzer, 1990). Only the former has the available space to accumulate large amounts of sucrose. A more detailed model of sucrose accumulation would be able to address this.

It has been proposed that phloem transport occurs mostly because of an osmotic pressure gradient along phloem tubes. This phenomenon is called the "Osmotically Generated Pessure Flow" (OGPF) model and was first described by Münch (1926, 1927, 1930). The pressure gradient results from solutes being loaded into the phloem at the source tissue and removed at the sink tissues. The hydrostatic pressure drives solutes from source to sink. Thompson and Holbrook (2003a) have published a theoretical model of this phenomenon and also provide a more

in-depth discussion of the OGPF model. The Thompson and Holbrook model has subsequently been analysed and compared to known data on phloem transport in a number of plant species (Thompson and Holbrook, 2003b, 2004; Thompson, 2005). If this proves to be correct and it is assumed that phloem unloading in sugarcane is primarily symplastic, then no significant sucrose concentrations would be expected in the parenchymal cytoplasm, because high cytoplasmic sucrose concentrations would destroy any osmotic pressure differences between sink and source tissue. Accumulation in the vacuole, or possibly even the apoplast, would be an absolute necessity if a constant flow of photosynthate and signalling molecules is to be achieved. It could be argued that solute concentrations in the cytoplasm should not increase. This would allow the maintenance, or possibly regulation of an osmotic pressure difference, in which case the model-predicted concentrations would be consistent with physiological concentrations. Unfortunately, no reliable data on solute compartmentation exists in parenchymal tissue.

4. Conclusion

The results presented here suggest that sucrose is not accumulated in the cytoplasm of the sugarcane storage parenchyma, but is rather transported into another compartment. The control of the flux split between sucrose accumulation and sucrose breakdown also does not shift drastically with the maturation of internodes; in fact, the majority of control resided in the same set of enzymes (i.e. Glc_{up}, Fru_{up}, VAC, HK_{Glc} and NI) in all eight internodes investigated. Finally, the futile cycling of sucrose seems to decrease as sugarcane internodes mature.

Acknowledgements

This work was funded by the National Bioinformatics Network (South Africa). We thank Brett Olivier for help with preparing model description files in SBML format.

Appendix A. Methods of analysis

A.1. Kinetic modelling of metabolism

One of the central aims of computational systems biology is to describe mathematically the dynamic behaviour of living organisms. The advantages of this approach are many; amongst others, it allows a formal, rigorous approach to be applied to biology. For example, within such a formalism, metabolism can be described as a highly parameterised system of enzyme catalysed reactions and, as a first approximation, such a system may be characterised by a set of ordinary differential equations (ODEs), termed a kinetic model of the system. Computational systems biology proceeds from the premise that by studying properties of the model we indirectly study the properties of the metabolic pathway concerned.

To briefly illustrate this approach, consider the following reaction scheme:

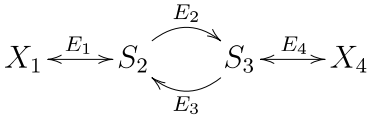

where X_1 and X_4 are external metabolites (source and sink), the concentrations of which are treated as constant. S_2 and S_3 are variable metabolites and E_1–E_4 are enzymes catalysing a particular step. The rate at which an enzyme catalyses a reaction can be described by an appropriate rate equation that, in this case, is a function of metabolite concentrations (substrates, products or effectors) and a set of parameters (e.g. Michaelis constants).

The topology of the above reaction scheme can be captured in matrix form,

$$\mathbf{N} = \begin{array}{c|cccc|c} & E_1 & E_2 & E_3 & E_4 & \\ \hline & 1 & -1 & 1 & 0 & S_2 \\ & 0 & 1 & -1 & -1 & S_3 \end{array} \tag{A.1}$$

where the elements of **N** are stoichiometric coefficients. Changes in metabolite concentrations are then given by,

$$\frac{\mathrm{d}\mathbf{S}}{\mathrm{d}t} = \mathbf{N}\mathbf{v} \tag{A.2}$$

where **S** and **v** are vectors of metabolites and rate equations, respectively. Eq. (A.2) effectively defines our system of ODEs, i.e. the kinetic model.

A.2. Steady-state solutions of a model

Frequently, biochemical pathways operate under conditions where the concentrations of the variable species and the fluxes through the reactions do not change significantly with time. Such a state is termed a (quasi-)steady-state. Kinetic models of pathways are very useful for steady-state analysis, since the solution to the system,

$$\mathbf{N}\mathbf{v} = \mathbf{0} \tag{A.3}$$

describes the steady-state concentrations and fluxes. Importantly, assuming a steady-state solution implies that the physiological interpretation of such a solution actually holds true, i.e. that rates and concentrations in a cell are in fact time-invariant. This assumption is certainly valid for small time scales, where drastic changes in state variables are unlikely to occur. Moreover, any particular

steady-state is only valid for a specific set of conditions. Cells are subjected to ever changing environments and if environmental conditions change, the conditions inside the cell change. This environmental change can be reflected in a change in the parameters that govern the kinetic model, which in turn will lead to a different steady-state solution. The concept of a quasi-steady-state deals with this issue: on small time scales fluxes and concentrations in a cell are in steady-state, but this steady-state itself changes over larger time scales. Steady-state solutions to a model thus provide a snapshot of conditions in a cell. The limitations of a steady-state as predicted by a model with static parameters should always be kept in mind, particularly its restriction to a single set of environmental conditions. In the current paper we deal with this issue by modelling every internode as a separate (quasi-)steady-state with unique parameters (Section 3.2). This assumption is reasonable considering that:

- Most validation data are in fact from steady-state experiments. For example, the experimental data used in the comparison in Fig. 3 are from flux measurements made in steady-state labelled sugarcane tissue discs.
- The temporal resolution for fluxes is in the order of minutes (model units are mM min^{-1}). It is expected that quasi-steady-state conditions should prevail under such short timescales, since growth rates are typically measured over months in sugarcane. Of course, on the longer time scale growth rates would not be expected to exhibit steady-state behaviour (e.g., sucrose accumulation is not a steady-state phenomenon). It is for this reason that we used kinetic parameter substitution to model growth.

A.3. Metabolic control analysis

Metabolic control analysis (MCA) is a steady-state framework, developed independently in the early 1970s by Kacser and Burns (1973) and Heinrich and Rapoport (1974), to quantify the extent to which individual reactions of a metabolic network control its state variables such as fluxes and metabolite concentrations (see Fell, 1996; Heinrich and Schuster, 1996 for more recent textbooks on MCA). Since the degree of control can be distributed among enzymes, MCA has superseded the long-standing concept of ''rate-limiting step''.

When a system of reactions is in steady-state, control coefficients can be calculated by altering an enzyme rate by a small amount (e.g. by varying a parameter that affects this step directly) and tracking the changes in all enzyme rates and species concentrations as the system settles into a new steady-state. Such a change is usually called a perturbation or modulation and the change in an enzyme rate or species concentration is a response.

A control coefficient is defined as the relative change in the state variable divided by the relative change in the activity of the affected step. Mathematically this can be expressed as

$$C_i^y = \frac{\partial \ln y}{\partial \ln v_i} = \frac{\partial y}{\partial v_i} \cdot \frac{v_i}{y} \tag{A.4}$$

where y is the state variable (concentration or flux) responding to the modulation, and v_i is the rate of an independent reaction step that is directly affected by the modulated parameter. A response coefficient directly quantifies the effect of a change in this model parameter on the state variable, and is defined as

$$R_p^y = C_i^y \times \varepsilon_p^i \tag{A.5}$$

where C_i^y is the control coefficient as defined in Eq. (A.4), and ε_p^i is an elasticity coefficient, which quantifies the local effect of the parameter on the rate of the perturbed reaction. It is defined as

$$\varepsilon_p^i = \frac{\partial \ln v_i}{\partial \ln p} \tag{A.6}$$

where v_i is the local reaction rate p is the modulated parameter.

A.4. Parameter scans

Kinetic models are extremely useful for analysing what would happen if one were to change a parameter through a range of possible values. For every value of the parameter, a new steady-state is calculated (the procedure is commonly termed ''parameter scanning''). It is therefore possible to characterise the response of a large number of fluxes and concentrations towards an ''*in silico*'' intervention that can be set up to mimic an experimental protocol in the laboratory (e.g., overexpressing an enzyme by different amounts).

A.5. Software

All calculations were performed on an IBM G40 Thinkpad personal computer with the PySCeS suite of cellular simulation software (http://pysces.sourceforge.net, Olivier et al., 2005). The programming language Python (http://www.python.org) was used for scripting routines not available in PySCeS, and the data were manipulated with the spreadsheet program Gnumeric (http://www.gnumeric.org), as described in Olivier et al. (2002) and Uys et al. (2006). PySCeS was used to calculate steady-states for different parameter sets, and to calculate the coefficients of MCA. The simulations were checked with the modelling programs Copasi (Hoops et al., 2006) and SBW (Sauro et al., 2003) and gave identical results in all cases.

Appendix B. Model parameter values

B.1. Maximal activities

We assumed that all reported enzyme activities are maximal activities; these are summarised in Table 3. All parameters are *in vitro* measurements. Most of the enzyme

activities change with internode maturity, but a subset was assumed to stay constant over all the internodes considered.

B.1.1. Activities that change with internode maturity

These activities restrict the model to the chosen internodes, i.e. 3–10, since enzymes from these are assayed most frequently. The experimental values used were usually reported as moles substrate converted per mass of total protein. A change in this quantity reflects a change in enzyme number. Changes in internode volume (S. Bosch, unpublished data) are accounted for in the conversion to our unit of choice, mM min^{-1}. This allows the extension of the model to various internodes since the specific activities reported in the literature are transformed into a profile of catalytic activity changes during internode maturation.

SuSy and FRK: The forward maximal velocities reported in Botha et al. (1996) measure the total activity of a specific reaction. As such, when isozymes are present, these values can be considered the weighted average value for the different isozymes. Therefore, we divided the overall value for FRK between FRK A and FRK B using the forward maximal velocity ratios in Hoepfner and Botha (2003), and the overall value for SuSy between SuSy A, B & C using the V_f/V_r ratios reported in Schäfer et al. (2004b).

UDPGDH: V_{UDPGDH} was estimated so that the steady-state flux to fibre as a fraction of glucose uptake matched *in vitro* flux measurements of Bindon and Botha (2002). Although a specific activity has been reported for UDPGDH in Turner and Botha (2002), measurements were only performed on immature tissue and a maximal activity profile could not be obtained.

B.1.2. Activities that stay constant with internode maturity

Vacuolar sucrose uptake: The vacuolar uptake step acts as a sink, hence it is irreversible. This is not implausible, since uptake can occur against a concentration gradient. No indication of saturation at physiological concentrations seems to exist (Preisser and Komor, 1991). Keeping the same maximal uptake rate of 1 mM min^{-1} as in the original model (Rohwer and Botha, 2001) ensured that the enzyme will not saturate and steady-state flux through the transporter could vary through a large range.

SPS and SPase: No internode-specific maximal activity values for SPase could be found. In this case the original value used by Rohwer and Botha (2001) for SPase was assumed to remain constant with internode maturity. SPS and SPase occur on the same branch, hence the steady-state flux through both enzymes will always be the same. SPase activity is higher than that of SPS for every internode, therefore steady-state flux through the branch can never be higher than the maximal activity of SPS. The control profile for both enzymes is also expected to be similar. Slight changes in the maximal activity of SPase therefore have virtually no effect on the model output. Together with SPase's irreversible rate equation, the assumption of a maximal velocity that does not change with internode maturity is thus warranted.

Table 4
Michaelis (*m*), half-saturation (0.5), inhibition (*i*) and equilibrium (*eq*) constants used in the model

Parameter	Value	Reference
Fru & Glc uptake		
K_m^{Fru} K_m^{Glc}	0.2	Rohwer and Botha (2001)
K_i^{Fru} K_i^{Glc}	1	
Hexokinase		
K_m^{Glc}	0.07	Rohwer and Botha (2001)
K_m^{ATP}	0.25	
K_m^{Fru}	10	
K_i^{G6P}	0.1	
K_i^{F6P}	10	
SPS		
K_{eq}	10	
K_i^{S6P}	0.07	Rohwer and Botha (2001)
$K_i^{P_i}$	3	
K_i^{UDPGlc}	1.4	
K_i^{F6P}	0.4	
K_m^{UDPGlc}	1.8	
K_m^{UDP}	0.3	
K_m^{S6P}	0.1	
K_m^{F6P}	0.6	
FRK		
$^{FRK\,A}K_m^{Fru}$	0.028	Hoepfner and Botha (2004)
$^{FRK\,B}K_m^{Fru}$	0.074	
$^{FRK\,A}K_m^{ATP}$	0.14	
$^{FRK\,B}K_m^{ATP}$	0.18	
$^{FRK\,B}K_i^{Fru}$	0.016	
Vacuolar Suc uptake		
K_m^{Suc}	100	Rohwer and Botha (2001)
NI		
K_i^{Glc}	15	Rohwer and Botha (2001)
K_i^{Fru}	15	
K_m^{Suc}	10	
UDPGDH		
K_m^{UDPGlc}	0.0187	Turner and Botha (2002)
K_m^{NAD+}	0.0722	
SuSy		
K_{eq}	0.5	Values for SuSy A & B were modified from Schäfer et al. (2005) to fit the Haldane relationship Parameters for SuSy C were obtained from Schäfer et al. (2004a)
$^{SuSy\,A}K_m^{Suc}$	22.51	
$^{SuSy\,A}K_m^{UDP}$	0.58	
$^{SuSy\,A}K_m^{UDPGlc}$	6.67	
$^{SuSy\,A}K_m^{Fru}$	12.29	
$^{SuSy\,B}K_m^{Suc}$	70.55	
$^{SuSy\,B}K_m^{UDP}$	0.14	
$^{SuSy\,B}K_m^{UDPGlc}$	0.82	
$^{SuSy\,B}K_m^{Fru}$	18.08	
$^{SuSy\,C}K_i^{UDP}$	0.0871	
$^{SuSy\,C}K_i^{Suc}$	1390	
$^{SuSy\,C}K_i^{Fru}$	3.1	
$^{SuSy\,C}K_m^{Suc}$	35.9	

Table 4 (*continued*)

Parameter	Value	Reference
${}^{\mathrm{SuSy\,C}}K_m^{\mathrm{Fru}}$	6.49	
${}^{\mathrm{SuSy\,C}}K_m^{\mathrm{UDP}}$	0.00191	
${}^{\mathrm{SuSy\,C}}K_m^{\mathrm{UDPGlc}}$	0.234	
PFK		
$\mathrm{F6P}_{0.5}$	0.758	Knowles et al. (1990)
$\mathrm{ATP}_{0.5}$	0.155	Cawood et al. (1988), Knowles et al. (1990), Turner and Plaxton (2003)
$\mathrm{ATP}_{0.5}^{\mathrm{modifier}}$	2	Estimate
h^{PFK}	2.3	Van Schaftingen et al. (1982)
σ	0.9	Estimate
Aldolase		
K_m^{FbP}	0.015	Brenda
PFP		
K_m^{F6P}	1	Kombrink et al. (1984), Kowalczyk et al. (1984), Mahajan and Singh (1989), Tripodi and Podesta (1997), Wong et al. (1988)
K_m^{FbP}	0.382	
$K_m^{\mathrm{PP}_i}$	0.12	
$K_m^{\mathrm{P}_i}$	0.51	
K_{eq}	3.3	Stitt (1990)
SPase		
K_m^{S6P}	0.1	Rohwer and Botha (2001)

Pre-superscripts indicate the specific isozyme, a post-superscript refers to the specific metabolite. Entries marked as Brenda were taken from the BRaunschweig ENzyme DAtabase (Schomburg et al., 2002, 2004).

B.2. Enzyme kinetic constants

Michaelis, half-saturation, inhibition and equilibrium constants are summarised in Table 4. Parameters which Ref. Rohwer and Botha (2001) are unchanged from our original model. Parameters for SuSy A & B were modified to adhere to the Haldane relationship (Cornish-Bowden, 1995),

$$K_{\mathrm{eq}} = \frac{V_{\mathrm{f}}}{V_{\mathrm{r}}}\frac{K_m^P K_m^Q}{K_m^A K_m^B} \tag{B.1}$$

where P,Q are products and A,B are substrates. V_{f} and V_{r} is the forward and reverse maximal activities, respectively. Substitution of the experimental values obtained from Schäfer et al. (2005) resulted in an inconsistency; calculating the equilibrium constant did not give 0.5, the value that it should be. The Michaelis constants were adjusted by introducing an error term,

$$\epsilon = \left(\frac{K_{\mathrm{eq}}^{\mathrm{app}}}{V_{\mathrm{f}}/V_{\mathrm{r}}}\right)^{\frac{1}{n}} \tag{B.2}$$

where $K_{\mathrm{eq}}^{\mathrm{app}}$ is the apparent K_{eq} obtained from the experimental data. Terms in the numerator were multiplied by ϵ and terms in the denominator were divided by ϵ. This approach was an attempt to distribute the error evenly between the Michaelis constants. The parameter n was fitted using a routine in Gnumeric; it does not have a physical meaning, but can be loosely interpreted as a measure of how far the experimental values deviate from the Haldane relationship. $n = 0.34$ for SuSy A and $n = 1.05$ for SuSy B. The parameters for SuSy C were left unchanged from the values used in Schäfer et al. (2004a) since they have already been adjusted to fit the Haldane relationship.

Table 5
Fixed concentration values of external metabolites and cofactors in the model

External metabolite/Cofactor	Clamped concentration (mM)
$\mathrm{Glc}_{\mathrm{apo}}$	5.0
$\mathrm{Fru}_{\mathrm{apo}}$	5.0
ATP	1.0
UDP	0.2
PP_i	0.2
P_i	5.1
NAD^+	1.0

Parameters for PFP and PFK were estimated from values extracted from BRENDA (Schomburg et al., 2002, 2004). Values reported for a particular parameter in various plants were averaged. The strength of the allosteric effect, σ, had to be estimated because no information on the value of this parameter could be found.

B.3. Constant concentrations of external metabolites and cofactors

The concentrations of the clamped external species as used in the model are summarised in Table 5. Note that the sink metabolites $\mathrm{Suc}_{\mathrm{vac}}$, UDPGA and TrP are not specified since the reactions leading up to them are irreversible, and their concentrations therefore do not enter into the model rate equations.

Appendix C. Rate equations

In the following we list only the rate equations for reactions that do not appear in the original model description of Rohwer and Botha (2001). The rate equations from the original model are used unchanged. If an equation (e.g. for FRK) or an enzyme mechanism (e.g. for UDPGDH) was specified by the relevant authors, this was used to simulate the reaction in our model. Alternatively, generic equations were used as specified below. Irreversible Michaelis–Menten equations with no product inhibition were only used for sink reactions (e.g. for ALD or VAC) where the product concentration is clamped and the reaction becomes *de facto* irreversible. When irreversible Michaelis–Menten equations were used for other reactions (e.g. NI or HK) that are not readily reversible, product inhibition term(s) were included (Cornish-Bowden, 1995). The only exception is SPase, which is present at high levels and has negligible flux or concentration control (other than on S6P; see also Appendix B.1). This

approach is in agreement with our previous model (Rohwer and Botha, 2001).

C.1. PFP

PFP catalyses the pyrophosphate-dependent phosphorylation of F6P to FbP

$$\mathrm{F6P} + \mathrm{PP}_i \rightleftharpoons \mathrm{FbP} + \mathrm{P}_i$$

and was modelled as a reversible two substrate two product Michaelis–Menten type rate equation assuming equilibrium binding of substrates and products.

$$v_{\mathrm{PFP}} = \frac{\frac{V_{\mathrm{PFP}}}{{}^{\mathrm{PFP}}K_m^{\mathrm{F6P}} \times {}^{\mathrm{PFP}}K_m^{\mathrm{PP}_i}}\left([\mathrm{F6P}][\mathrm{PP}_i] - \frac{[\mathrm{FbP}][\mathrm{P}_i]}{{}^{\mathrm{PFP}}K_{\mathrm{eq}}}\right)}{\left(1 + \frac{[\mathrm{F6P}]}{{}^{\mathrm{PFP}}K_m^{\mathrm{F6P}}} + \frac{[\mathrm{FbP}]}{{}^{\mathrm{PFP}}K_m^{\mathrm{FbP}}}\right)\left(1 + \frac{[\mathrm{PP}_i]}{{}^{\mathrm{PFP}}K_m^{\mathrm{PP}_i}} + \frac{[\mathrm{P}_i]}{{}^{\mathrm{PFP}}K_m^{\mathrm{P}_i}}\right)} \tag{C.1}$$

C.2. PFK

Phosphofructokinase was modelled as a two-substrate Hill-type equation (Hanekom, 2006; Hanekom et al., 2006)

$$\mathrm{F6P} + \mathrm{ATP} \rightarrow \mathrm{FbP} + \mathrm{ADP}$$

$$v_{\mathrm{PFK}} = \frac{V_{\mathrm{PFK}}\alpha\beta}{\frac{1+\mu}{1+\sigma^{4h}\mu} + \frac{(\alpha+\beta)(1+\sigma^{2h}\mu)}{1+\sigma^{4h}\mu} + \alpha\beta}$$

$$\text{where} \quad \alpha = \left(\frac{[\mathrm{F6P}]}{\mathrm{F6P}_{0.5}}\right)^h$$

$$\beta = \left(\frac{[\mathrm{ATP}]}{\mathrm{ATP}_{0.5}}\right)^h$$

$$\mu = \left(\frac{[\mathrm{ATP}]}{\mathrm{ATP}_{0.5}^{\mathrm{modifier}}}\right)^h$$

σ = coefficient of allosteric modification

C.3. ALD

The aldolase reaction was described by an irreversible Michaelis–Menten mechanism.

$$\mathrm{FbP} \rightarrow 2\mathrm{TrP}$$

$$v_{\mathrm{ALD}} = \frac{V_{\mathrm{ALD}}[\mathrm{FbP}]}{{}^{\mathrm{ALD}}K_m^{\mathrm{FbP}} + [\mathrm{FbP}]} \tag{C.2}$$

C.4. SuSy

SuSy was modelled with a reversible bi-substrate Michaelis–Menten equation,

$$\mathrm{UDPGlc} + \mathrm{Fru} \rightleftharpoons \mathrm{Suc} + \mathrm{UDP}$$

$$v_{\mathrm{SuSy\,A,B}} = \frac{\frac{-V_{\mathrm{SuSy\,A,B}}}{{}^{\mathrm{SuSy\,A,B}}K_m^{\mathrm{Suc}} \times {}^{\mathrm{SuSy\,A,B}}K_m^{\mathrm{UDP}}}\left([\mathrm{UDP}][\mathrm{Suc}] - \frac{[\mathrm{Fru}][\mathrm{UDPGlc}]}{{}^{\mathrm{SuSy}}K_{\mathrm{eq}}}\right)}{\left(1 + \frac{[\mathrm{UDPGlc}]}{{}^{\mathrm{SuSy\,A,B}}K_m^{\mathrm{UDPGlc}}} + \frac{[\mathrm{UDP}]}{{}^{\mathrm{SuSy\,A,B}}K_m^{\mathrm{UDP}}}\right)\left(1 + \frac{[\mathrm{Fru}]}{{}^{\mathrm{SuSy\,A,B}}K_m^{\mathrm{Fru}}} + \frac{[\mathrm{Suc}]}{{}^{\mathrm{SuSy\,A,B}}K_m^{\mathrm{Suc}}}\right)} \tag{C.3}$$

where $V_{\mathrm{SuSy\,A,B}}$ are the maximal velocities of SuSy A & B, K_m^S are Michaelis constants with respect to metabolite S, and ${}^{\mathrm{SuSy}}K_{\mathrm{eq}}$ is the equilibrium constant for the reaction. $V_{\mathrm{SuSy\,A,B}}$ and ${}^{\mathrm{SuSy}}K_{\mathrm{eq}}$ are defined in terms of the *sucrose breakdown* reaction (the enzyme is most commonly assayed in this direction). However, the model reaction is defined in the direction of *sucrose synthesis*. In keeping with the approach of Rohwer and Botha (2001), the negative sign was prepended to cast the model in terms of positive steady-state fluxes.

C.5. FRK

Fructokinase only phosphorylates fructose as opposed to hexokinase, which takes both Glc and Fru as substrates.

$$\mathrm{Fru} + \mathrm{ATP} \rightarrow \mathrm{F6P} + \mathrm{ADP}$$

This enzyme occurs as two known isozymes, labeled FRK A & B. The rate equations from the original enzyme characterisation (Hoepfner and Botha, 2003, 2004) were used to model the respective catalytic steps

$$v_{\mathrm{FRK\,A}} = \frac{V_{\mathrm{FRK\,A}}[\mathrm{Fru}][\mathrm{ATP}]}{{}^{\mathrm{FRK\,A}}K_m^{\mathrm{ATP}}[\mathrm{Fru}] + {}^{\mathrm{FRK\,A}}K_m^{\mathrm{Fru}}[\mathrm{ATP}] + [\mathrm{Fru}][\mathrm{ATP}]} \tag{C.4}$$

$$v_{\mathrm{FRK\,B}} = \frac{V_{\mathrm{FRK\,B}}[\mathrm{Fru}][\mathrm{ATP}]}{{}^{\mathrm{FRK\,B}}K_m^{\mathrm{ATP}}[\mathrm{Fru}] \times \left(1 + \frac{[\mathrm{Fru}]}{{}^{\mathrm{FRK\,B}}K_i^{\mathrm{Fru}}}\right) + {}^{\mathrm{FRK\,B}}K_m^{\mathrm{Fru}}[\mathrm{ATP}] + [\mathrm{Fru}][\mathrm{ATP}]} \tag{C.5}$$

C.6. UDPGDH

The inclusion of UDPGDH in the model introduces a third possible route that carbohydrates can follow in the sugarcane culm. This is a four-electron transfer reaction with the following net stoichiometry:

$$\mathrm{UDPGlc} + 2\mathrm{NAD}^+ \rightarrow \mathrm{UDPGA} + 2\mathrm{NADH}$$

UDPGA is the precursor to pectin and hemicellulose, which in turn are the building blocks of extracellular matrix polysaccharides (Turner and Botha, 2002). Storage and respiration are already accounted for in the model and this reaction ensures that the hexose phosphate pool can be used for fibre formation. UDPGDH was modelled as an irreversible bi-uni-uni-bi reaction (Turner and Botha, 2002), using a three substrate Michaelis–Menten equation (Cornish-Bowden, 1995)

$$\begin{aligned} v_{\mathrm{UDPGDH}} = {} & \frac{V_{\mathrm{UDPGDH}}[\mathrm{UDPGlc}][\mathrm{NAD}^+]^2}{{}^{\mathrm{UDPGDH}}K_m^{\mathrm{UDPGlc}} \times {}^{\mathrm{UDPGDH}}K_m^{\mathrm{NAD}^+}[\mathrm{NAD}^+]} \\ & + 2\left({}^{\mathrm{UDPGDH}}K_m^{\mathrm{NAD}^+}[\mathrm{UDPGlc}][\mathrm{NAD}^+]\right) \\ & + {}^{\mathrm{UDPGDH}}K_m^{\mathrm{UDPGlc}}[\mathrm{NAD}^+]^2 + [\mathrm{UDPGlc}] \\ & \times [\mathrm{NAD}^+]^2. \end{aligned} \tag{C.6}$$

References

Bindon, K., Botha, F., 2002. Carbon allocation to the insoluble fraction, respiration and triose-phosphate cycling in the sugarcane culm. Physiol. Plantarum 116, 12–19.

Bosch, S., 2005. Trehalose and carbon partitioning in sugarcane. Ph.D. thesis, University of Stellenbosch.

Bosch, S., Grof, C., Botha, F., 2004. Expression of neutral invertase in sugarcane. Plant Sci. 166, 1125–1133.

Botha, F.C., Black, K.G., 2000. Sucrose phosphate synthase and sucrose synthase activity during maturation of internodal tissue in sugarcane. Aust. J. Plant Physiol. 27, 81–85.

Botha, F.C., Whittaker, A., Vorster, D.J., Black, K.G., 1996. Sucrose accumulation rate, carbon partitioning and expression of key enzyme activities in sugarcane stem tissue. In: Wilson, J.R., Hogarth, D.M., Campbell, J.A., Garside, A.L. (Eds.), Sugarcane: Research Towards Efficient and Sustainable Production. CSIRO division of Tropical Crops and Pastures, Brisbane, pp. 98–101.

Cawood, M., Botha, F., Small, J., 1988. Properties of the phosphofructokinase isoenzymes from germinating cucumber seeds. J. Plant Physiol. 132, 204–209.

Cornish-Bowden, A., 1995. Fundamentals of Enzyme Kinetics. Portland Press, London.

Fell, D.A., 1996. Understanding the Control of Metabolism. Portland Press, London.

Glasziou, K., 1960. Accumulation and transformation of sugars in sugar cane stalks. Plant Physiol., 895–901.

Hanekom, A.J., 2006. Generic kinetic equations for modelling multisubstrate reactions in computational systems biology. Master's thesis, Stellenbosch University.

Hanekom, A.J., Hofmeyr, J.-H.S., Snoep, J.L., Rohwer, J.M., 2006. Experimental evidence for allosteric modifier saturation as predicted by the bi-substrate hill equation. IEE Proc.-Syst. Biol. 153 (5), 342–345.

Hatch, M.D., Glasziou, K.T., 1963. Sugar accumulation cycle in sugar cane II: relationship of invertase activity to sugar content and growth rate storage tissue of plants grown in controlled environments. Plant Physiol. 38, 344–348.

Heinrich, R., Rapoport, T.A., 1974. A linear steady-state treatment of enzymatic chains. General properties, control and effector strength. Eur. J. Biochem. 42, 89–95.

Heinrich, R., Schuster, S., 1996. The Regulation of Cellular Systems. Chapman & Hall, New York.

Hoepfner, S.W., Botha, F.C., 2003. Expression of fructokinase isoforms in the sugarcane culm. Plant Physiol. Biochem. 41, 741–747.

Hoepfner, S.W., Botha, F.C., 2004. Purification and characterisation of fructokinase from the culm of sugarcane. Plant Sci. 167, 645–654.

Hoops, S., Sahle, S., Gauges, R., Lee, C., Pahle, J., Simus, N., Singhal, M., Xu, L., Mendes, P., Kummer, U., 2006. COPASI – a COmplex PAthway SImulator. Bioinformatics 22 (24), 3067–3074.

Kacser, H., Burns, J.A., 1973. The control of flux. Symp. Soc. Exp. Biol. 27, 65–104.

Knowles, V., Greyson, M., Dennis, D., 1990. Characterization of ATP-dependent fructose 6-phosphate 1-phosphotransferase isozymes from leaf and endosperm tissues of Ricinus communis. Plant Physiol. 92, 155–159.

Kombrink, E., Kruger, N., Beevers, H., 1984. Kinetic properties of pyrophosphate:D-fructose-6-phosphate phosphotransferase from germinating castor bean endosperm. Plant Physiol. 74, 395–401.

Komor, E., 1994. Regulation by futile cycles: the transport of carbon and nitrogen in plants. In: Schulze, E.D. (Ed.), Flux Control in Biological Systems. Academic Press, San Diego, pp. 153–201.

Komor, E., 2000a. The physiology of sucrose storage in sugarcane. In: Gupta, A.K., Kaur, N. (Eds.), Carbohydrate Reserves in Plants – Synthesis and Regulation. Elsevier Science, Amsterdam, pp. 35–54.

Komor, E., 2000b. Source physiology and assimilate transport: the interaction of sucrose metabolism, starch storage and phloem export in source leaves and the effect on sugar status in phloem. Aust. J. Plant Physiol. 27, 497–505.

Komor, E., Thom, M., Maretzki, A., 1981. The mechanism of sugar uptake by sugarcane suspension cells. Planta 153, 181–192.

Kowalczyk, S., Januszewska, B., Cymerska, E., Maslowski, P., 1984. The occurence of inorganic pyrophosphate:D-fructose-6-phosphate 1-phosphotransferase in higher plants I: Initial characterization of partially purified enzyme from *Sanseviera trifasciata* leaves. Physiol. Plantarum 60, 31–37.

Ma, H., Albert, H., Paull, R., Moore, P., 2000. Metabolic engineering of invertase activities in different subcellular compartments affects sucrose accumulation in sugarcane cells. Aust. J. Plant Physiol. 27, 1021–1030.

Mahajan, R., Singh, R., 1989. Properties of pyrophosphate:D-fructose-6-phosphate phosphotransferase from endosperm of developing wheat (*Triticum aestivum* L.) grains. Plant Physiol. 91, 421–426.

Moore, P.H., 1995. Temporal and spatial regulation of sucrose accumulation in the sugarcane. Aust. J. Plant Physiol. 22, 661–679.

Moore, P.H., Maretzki, A., 1996. Sugarcane. In: Zamski, E., Schaffer, A.A. (Eds.), Photoassimilate Distribution in Plants and Crops: Source-Sink Relationships. Marcel Dekker Inc., New York, pp. 643–669.

Münch, E., 1926. Über Dynamik der Saftströmungen. Ber. Deut. Bot. Ges. 44, 68–71.

Münch, E., 1927. Versuche über den Saftkreislauf. Ber. Deut. Bot. Ges. 45, 340–356.

Münch, E., 1930. Die Stoffbewegungen in der Pflanze, vol. 45, Jena: Gustav Fischer.

Olivier, B.G., Rohwer, J.M., Hofmeyr, J.-H.S., 2002. Modelling cellular processes with Python and SciPy. Mol. Biol. Rep. 29, 249–254.

Olivier, B.G., Rohwer, J.M., Hofmeyr, J.-H.S., 2005. Modelling cellular systems with PySCeS. Bioinformatics 21 (4), 560–561.

Prado, F.E., Fleischmacher, O.L., Vattuone, M.A., Sampietro, A.R., 1980. Cell wall invertases of sugar cane. Phytochemistry 21 (12), 2825–2828.

Preisser, J., Komor, E., 1991. Sucrose uptake into vacuoles of sugarcane suspension cells. Planta (Historical Archive) 186 (1), 109–114.

Rae, A.L., Perroux, J.M., Grof, C.P.L., 2005. Sucrose partitioning between vascular bundles and storage parenchyma in the sugarcane stem: a potential role for the ShSUT1 sucrose transporter. Planta 220 (6), 817–825.

Rohwer, J.M., Botha, F.C., 2001. Analysis of sucrose accumulation in the sugar cane culm on the basis of *in vitro* kinetic data. Biochem. J. 358, 437–445.

Rose, S., Botha, F., 2000. Distribution patterns of neutral invertase and sugar content in sugarcane internodal tissues. Plant Physiol. Biochem. 38, 819–824.

Sauro, H.M., Hucka, M., Finney, A., Wellock, C., Bolouri, H., Doyle, J., Kitano, H., 2003. Next generation simulation tools: the Systems Biology Workbench and BioSPICE integration. OMICS 7 (4), 355–372.

Schäfer, W.E., Rohwer, J.M., Botha, F.C., 2004a. A kinetic study of sugarcane sucrose synthase. Eur. J. Biochem. 271, 3971–3977.

Schäfer, W.E., Rohwer, J.M., Botha, F.C., 2004b. Protein-level expression and localization of sucrose synthase in the sugarcane culm. Physiol. Plantarum 121, 187–195.

Schäfer, W.E., Rohwer, J.M., Botha, F.C., 2005. Partial purification and characterisation of sucrose synthase in sugarcane. J. Plant Physiol. 162, 11–20.

Schomburg, I., Chang, A., Ebeling, C., Gremse, M., Heldt, C., Huhn, G., Schomburg, D., 2004. BRENDA, the enzyme database: updates and major new developments. Nucleic Acids Res. 32 (Database issue), D431–D433.

Schomburg, I., Chang, A., Hofmann, O., Ebeling, C., Ehrentreich, F., Schomburg, D., 2002. BRENDA: a resource for enzyme data and metabolic information. Trends Biochem. Sci. 27 (1), 54–56.

Stitt, M., 1990. Fructose-2,6-bisphosphate as a regulatory molecule in plants. Annu. Rev. Plant Physiol. Plant. Mol. Biol. 41, 153–185.

Thompson, M., 2005. Scaling phloem transport: elasticity and pressure-concentration waves. J. Theor. Biol. 236, 229–241.

Thompson, M., Holbrook, N., 2003a. Application of a single-solute non-steady-state phloem model to the study of long distance assimilate transport. J. Theor. Biol. 220, 419–455.

Thompson, M., Holbrook, N., 2003b. Scaling phloem transport: water potential equilibrium and osmoregulatory flow. Plant Cell Environ. 26, 1561–1577.

Thompson, M., Holbrook, N., 2004. Scaling phloem transport: information transmission. Plant Cell Environ. 27, 509–519.

Titus, C., 2005. Sucrose transporters and sucrose uptake mechanisms in sugarcane. Master's thesis, University of Stellenbosch.

Tripodi, K., Podesta, F., 1997. Purification and structural and kinetic characterization of the pyrophosphate:fructose-6-phosphate 1-phosphotransferase from the crassulacean acid metabolism plant, pineapple. Plant Physiol. 113, 779–786.

Turner, W., Botha, F.C., 2002. Purification and kinetic properties of UDP-glucose dehydrogenase from sugarcane. Arch. Biochem. Biophys. 407 (2), 209–216.

Turner, W., Plaxton, W., 2003. Purification and characterization of pyrophosphate- and ATP-dependent phosphofructokinases from banana fruit. Planta 217, 113–121.

Uys, L., 2006. Computational systems biology of sucrose accumulation in sugarcane. Master's thesis, University of Stellenbosch.

Uys, L., Hofmeyr, J.-H., Snoep, J., Rohwer, J., 2006. Software tools that facilitate kinetic modelling with large data sets: an example using growth modelling in sugarcane. IEE Proc.-Syst. Biol. 153 (5), 385–389.

Van Schaftingen, E., Lederer, B., Bartrons, R., Hers, H.-G., 1982. A kinetic study of pyrophosphate: fructose-6-phosphate phosphotransferase from potato tubers. Eur. J. Biochem. 129, 191–195.

Vattuone, M.A., Prado, F.E., Sampietro, A.R., 1981. Cell wall invertases from sugar cane. Phytochemistry 20 (2), 189–191.

Venkataramana, S., Naidu, K.M., Singh, S., 1991. Invertases and growth factors dependent sucrose accumulation in sugarcane. Plant Sci. 74 (1), 65–72.

Vorster, D.J., Botha, F.C., 1998. Partial purification and characterisation of sugarcane neutral invertase. Phytochemistry 49, 651–655.

Vorster, D.J., Botha, F.C., 1999. Sugarcane internodal invertases and tissue maturity. J. Plant Physiol. 155, 470–476.

Walsh, K., Sky, R., Brown, S., 2005. The anatomy of the pathway of sucrose unloading within the sugarcane stalk. Funct. Plant Biol. 32, 367–374.

Welbaum, G., Meinzer, F., 1990. Compartmentation of solutes and water in developing sugarcane stalk in tissue. Plant Physiol. 93, 1147–1153.

Whittaker, A., Botha, F.C., 1997. Carbon partitioning during sucrose accumulation in sugarcane internodal tissue. Plant Physiol. 115, 1651–1659.

Wong, J., Kang, T., Buchanan, B., 1988. A novel pyrophosphate D-fructose-6-phosphate 1-phosphotransferase from carrot roots: relation to PFK from the same source. FEBS Lett. 238, 405–410.

Zhu, Y.J., Komor, E., Moore, P.H., 1997. Sucrose accumulation in the sugarcane stem is regulated by the difference between the activities of soluble acid invertase and sucrose phosphate synthase. Plant Physiol. 115, 609–616.